JCMT SCUBA-DIVING IN NEARBY MOLECULAR CLOUDS: THE CASE FOR LARGE SYSTEMATIC SURVEYS WITH FIRST

D. Johnstone

Department of Astronomy, University of Toronto, Toronto, Ontario, M5S 3H8, Canada

Abstract

Results from two sub-millimeter surveys of the nearby molecular clouds ρ Oph, Taurus, Orion A and Orion B are presented. Combining large area (100's of square arcminute) JCMT continuum emission images at 450μm (8") and 850μm (14"), sensitive to $\sim 0.01\,M_\odot$ condensations, with molecular line data (CO isotopes, formaldehyde, etc.) allows for a glimpse into the physical properties of molecular clouds on small scales. Both barely resolved condensations and large scale features are visible in the maps, revealing the variety of dynamical events which operate in star forming regions. The important physics associated with these regions, as evidenced by the survey results, are discussed. Equilibrium Bonnor-Ebert models are fit to the compact clumps found in the dust continuum images in order to derive their physical properties - mass, temperature, and bounding pressure. The cumulative mass functions for the clumps in both Orion B and ρ Oph are remarkably similar to the stellar IMF. The survey results are used to argue for a strong multi-wavelength and multi-instrument survey component to the FIRST mission in order to best unlock the secrets of star formation in molecular clouds.

Key words: Stars: formation – Missions: FIRST

1. Introduction

The quality of data obtained with the new generation of bolometer instruments is such that we can now probe structure within molecular clouds at stellar mass scales. Combining this sensitivity with large-area mapping techniques and complimentary molecular line observations allows for a more detailed examination of the range of physical conditions present at the start of star formation.

This paper summarizes the results of two on-going surveys of molecular clouds: a study into Orion A by Johnstone and Bally (Johnstone & Bally 1999), and a larger multi-cloud Canadian JCMT key project (Wilson et al. 1999; Johnstone et al. 2000b; Johnstone et al. 2001; and Mitchell et al. 2001). Both surveys use the bolometer array SCUBA (Holland et al. 1999) at the JCMT to produce large-area, 100's of arc-minutes, maps of dense regions within these nearby molecular clouds in order to observe the structures down to small scales. SCUBA operates simultaneously at both 450μm and 850μm producing high sensitivity (rms noise ~ 0.01 Jy per beam at 850μm) scan-maps with reasonable spatial resolution (14" at 850μm). Assuming standard dust properties within the molecular cloud and a dust temperature of $\sim$ 20K, this flux corresponds to a gas column density of $\sim 10^{21}\mathrm{cm}^{-2}$ ($A_v \sim 1$). At the distance of Orion the total mass associated with an integrated flux of 1 Jy at 850μm is $\sim 1M_\odot$ while at the much closer distance of ρ Oph this integrated flux yields $\sim 0.1M_\odot$. Thus, the sensitivity of the surveys probe the entire stellar mass range of clumps. Unfortunately, ground based observations must overcome atmospheric fluctuations and thus instead of direct measurements of the sky the data is obtained as a difference (chopped) map. Reconstructing the image (Johnstone et al. 2000a) is a complicated procedure that has very limited success at recovering large-scale features suppressed by the chop. As such, despite the large-area of the survey maps, most of the structure observed is the small scale fragmentation of the cloud and it is difficult to make strong claims about larger features. FIRST should yield considerable progress on these larger scales, where the higher sensitivity and stability of a satellite above the atmosphere will allow for much more extensive mapping.

2. Orion A

One of the first large-area maps observed with SCUBA was the Integral Shaped Filament in the Orion A molecular cloud (Johnstone & Bally 1999). Figure 1 presents the 850μm data using both linear and logarithmic intensity maps. Aside from the fragmented but otherwise continuous filament stretching north-south and coincident with the molecular filament (Bally et al. 1987), four obvious sub-regions are identifiable: the OMC 1 molecular cloud core at the center of the map; FIR4, coincident with the OMC 2 molecular cloud core; MMS6, coincident with the OMC 3 molecular cloud core; and the double-stranded fainter region south of OMC 1 which we designate OMC 4. Within this large-scale structure are smaller filaments: dust shells from the swept up walls of the expanding HII regions M42 and M43, and fingered dust filaments radiating from OMC 1 and coincident with dense ammonia (Wiseman & Ho 1998) formed either through fragmentation of the molecular core or sculpted by the known out-

Proc. Symposium *'The Promise of the Herschel Space Observatory'* 12–15 December 2000, Toledo, Spain
ESA SP-460, July 2001, eds. G.L. Pilbratt, J. Cernicharo, A.M. Heras, T. Prusti, & R. Harris

flows from the core center. The ridge breaks into dozens of clumps at small scales, with individual masses similar to stellar masses. The location of the clumps observed at 850μm along the ridge peak in OMC 2 and 3 is in excellent agreement with the clumps discovered at 1.3mm with IRAM by Chini et al. (1997).

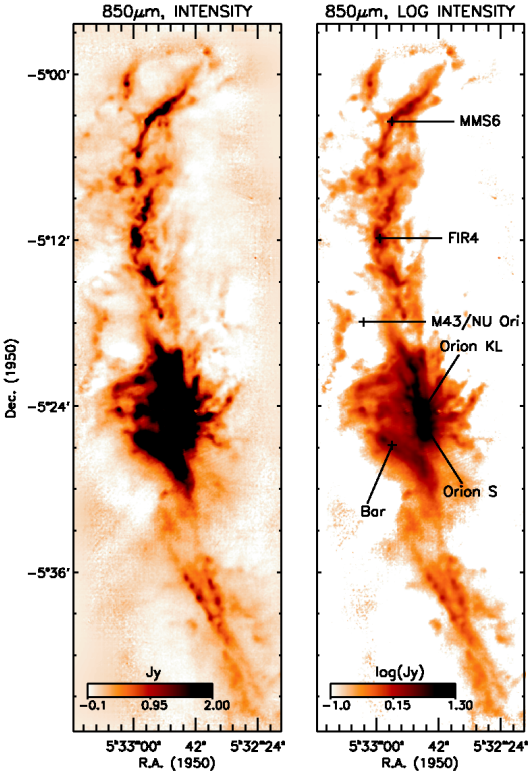

Figure 1. The 850μm emission from the ISF at the northern end of the Orion A Molecular cloud. Left Panel: linear transfer function. Right Panel: logarithmic transfer function.

Given superb weather conditions when the Orion A map was obtained, the quality of the 450μm map was high enough that comparison between the two wavelengths is possible. The spectral index, γ, of each location within the ridge was computed assuming that $S_\nu \propto \nu^\gamma$ and was found to vary between $2.0 < \gamma < 4.5$. For optically thin dust emission at a constant temperature the observed flux should be proportional to the Planck function $B_\nu(T)$ multiplied by the optical depth, which varies with frequency as the dust opacity $\kappa_\nu \propto \nu^\beta$. For high temperatures $T > 50\,\mathrm{K}$ the emission falls in the Raleigh-Jeans tail of the Planck function where $B_\nu \propto \nu^2$; however, at lower temperatures the effective power-law index is smaller. Separating the effects of temperature and changes in the dust opacity power-law are difficult without further information but the mean spectral index $\gamma \sim 3.5$ within the map is well fit by a dust temperature of 30K and a $\beta \sim 2$.

Within the denser clumps the spectral index decreases, indicating a lower temperature, a change in the dust properties $\beta < 2$, or both conditions. One extra concern when producing these spectral index maps is the degree to which lines contaminate the broadband flux measurements. In the embedded source, Orion-KL at the center of OMC 1, contamination from molecular lines, especially SO and SO_2, occurs within the 850μm broadband at about the fifty percent level (Groesbeck 1994; Serabyn & Weisstein 1995). Recent molecular line observations (Johnstone 2001) of a particular 850μm clump (peak flux 0.4 Jy per beam) in the Orion A map coincident with an H_2 shock feature (Yu et al. 1997) reveals that about 80% of the broadband flux in this feature is due to enhanced CO and ^{13}CO emission from the broad (> 20km/s) shock line width.

Determining the detailed properties of the clumps is complicated by the fact that they are embedded in the larger structure of the filament and separation of these two components is not simple. Thus, the analysis of Orion A has concentrated on the structure of the underlying ridge. Dividing the ridge into three components, OMC 1-3, the average intensity orthogonal to the ridge for each region shows remarkable similarity. The profiles are well fit by a power-law distribution with $S(R) \propto R^{-\alpha}$, where $\alpha \sim 1$ for $R < 100$". Further from the ridge the measurements are complicated by the inability of difference maps to measure large-scale structure. Assuming a constant temperature and dust emissivity model for the ridge, the intensity profile is proportional to the column density and the ridge profile can be compared with a self-gravitating isothermal cylinder model (Ostriker 1964). Neither the finite core radius nor the steep $\alpha = 3$ power-law column density profile of such an equilibrium structure is observed. However the profile is consistent with recent models of molecular filaments supported and constrained by helical magnetic fields (Fiege & Pudritz 2000a). SCUBA polarimetry observations of OMC 3 by Matthews & Wilson (2000) appear to support this model (Fiege & Pudritz 2000c). Within the observed ridge there are multiples scales of fragmentation (1.3pc, 0.3pc, 0.1pc). Fiege & Pudritz 2000b suggest that the largest fragmentation scale is reproduced through linear growth of instabilities in the helical model but an important test will be whether all scales can be reproduced during a more extensive evolution of helical filaments.

FIRST should have a great advantage in determining large-scale structure within molecular clouds. The ability to measure directly the spectral energy distribution will aid in separating temperature and dust emissivity changes throughout the cloud, allowing for a detailed look at the underlying physical conditions.

3. Clumps in ρ Oph, Orion B, and Taurus

A great deal of effort has been devoted to obtaining physical information about the clumps observed in the dust emission maps. The most rigorous measurement is that of

clump mass (although the mass determinations are subject to temperature and dust emissivity uncertainties it is expected that these produce uncertainties in the derived masses of less than a factor of 2). Motte et al. (1998) measured the masses of clumps within ρ Oph from 1.3mm observations taken at IRAM and found a distribution of masses similar to the stellar initial mass function (IMF). Testi & Sargent (1998) found a similar distribution for clumps within the Serpens molecular cloud using OVRO at 3mm.

The high sensitivity of SCUBA, combined with the reasonable resolution (15" beam at 850μm) of the JCMT, is ideally suited to the task of obtaining measurements of stellar mass clumps. The Canadian key project(Wilson et al. 1999, Johnstone et al. 2000b, Johnstone et al. 2001) has obtained ~ 1000 arcmin^2 maps of star-forming regions within ρ Oph, Orion B, and Taurus. Using a standardized recipe to reduce the data and measure clump properties, comparison of the survey results across clouds is possible. To identify and measure the observational properties of the clumps the clump-finding algorithm *clfind* by Williams et al. (1994) is used. The clumps are then associated with isothermal Bonnor-Ebert spheres (Ebert 1955, Bonnor 1956) allowing for a transformation from the angular size, integrated flux, and concentration of each clump into the physical properties of internal temperature, total mass, and bounding pressure.

In ρ Oph fifty-five clumps were obtained spanning the stellar mass range ($0.02 < M/M_\odot < 2.4$). The Bonnor-Ebert analysis suggests that the clumps have internal temperatures in the range $10\mathrm{K} < T < 30\mathrm{K}$ and that the bounding pressure on each clump lies in the range $P/k = 10^{6-7}\,\mathrm{K\ cm^{-3}}$, consistent with the expected equilibrium pressure in the ρ Oph central region (Johnstone et al. 2000b). The cumulative mass spectrum in Figure 2 reproduces the Motte et al. (1998) stellar IMF-like distribution of clumps; however, while both clump mass functions show a flattening at low masses ($< 0.5 M_\odot$) it is unclear whether this is due to completeness effects. Johnstone et al. (2000b) suggest that incompleteness occurs at much higher masses than Motte et al. estimate.

In Orion B, specifically the NGC 2068, NGC 2071, and HH 24-26 region in the northern part of the cloud, seventy-five clumps were obtained spanning the mass range ($0.2 < M/M_\odot < 12.3$). The Bonnor-Ebert analysis suggests somewhat higher temperatures than in ρ Oph, $20\mathrm{K} < T < 40\mathrm{K}$, perhaps due to the enhanced interstellar radiation field in the Orion region. As well, the required bounding pressure on the clumps is somewhat lower than in ρ Oph, $P/k = 10^{5.5-6.5}\,\mathrm{K\ cm^{-3}}$ in agreement with the lower expected equilibrium pressure at the center of the Orion B cloud (Johnstone et al. 2001). The cumulative mass spectrum is slightly steeper than that found in ρ Oph but is in general agreement with a stellar IMF. Again, a flattening is observed at low masses although the mass of the turn-over is higher than in ρ Oph, as expected if the turn-over is due to completeness and given the larger distance to Orion B.

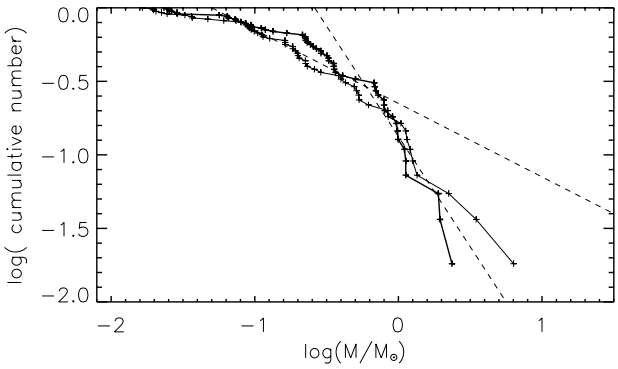

Figure 2. Cumulative mass function for clumps with masses greater than M. The thin line converts the measured integrated flux for each clump using a constant 20 K temperature. The thick line converts using the temperature derived from Bonnor-Ebert fitting. The shallow dashed line has a slope $M^{-0.5}$ while the steep dashed line has a slope of $M^{-1.5}$ approximating the IMF.

The results from these two molecular clouds suggest that the clumps are the starting point for star-formation, and that determination of the stellar IMF occurs at an early stage of fragmentation (from which the observed clumps were produced). It is interesting to note however that while a large region of Taurus has been mapped, there have been few if clumps observed.

While stable equilibrium Bonnor-Ebert models provide reasonable fits to the clump data they also raise an important question. If the clumps are indeed in equilibrium, how do they become unstable and collapse? Three possible solutions present themselves: the clump temperature decreases significantly, the clump mass increases through accretion, or the bounding pressure on the clump increases. Combining molecular line data and the nearly complete spectral energy coverage available with FIRST will allow much more detailed models of the clumps to be developed. The sensitivity of FIRST will provide additional constraints on the regions within which the clumps are embedded perhaps tying the clumps back to the prenatal molecular cloud cores.

Given the non-random distribution of clumps in both the ρ Oph and Orion B maps it is useful to consider the clustering scale of these sources. By measuring the two-point correlation function, both the strength of the clustering and the linear scale r_0 of the clustering is obtained. Both molecular clouds show the same strength of clustering, coincidentally similar to the strength of clustering observed in the angular separation of Galaxies, while the linear scale over which the clustering occurs is 0.15 pc in ρ Oph (Johnstone et al. 2000b) and 0.75 pc in Orion B

(Johnstone et al. 2001). Both these length scales are *larger* than the thermal Jeans length in the respective clouds but *smaller* than the Jeans length if the observed turbulent motions deduced from the typical molecular line widths within the parent cloud are included. As well, considering the mean density within each region, the column density through the clump clusters is $N_{H_2} \sim 10^{22}\mathrm{cm}^{-2}$ which yields an $A_v \sim 4-10$. McKee (1989) has suggested that such a column density may isolate the interiors of molecular clouds from diffuse far-ultraviolet radiation and thus allow the clouds to cool efficiently. Myers & Lazarian (1998) additionally consider the loss of non-thermal support due to the decay of magnetic fields in such regions. Essentially the ionization of these coherent regions is lower than in the surroundings due to the small number of energetic photons that are able to penetrate. Since the thermal support is not enough to hold up the region, once the non-thermal support dissipates the cloud collapses and fragments. It remains to be determined if such a collapse is capable of producing the clumps observed in the SCUBA maps.

4. Dust and Gas Comparison in Orion B

A comparison between the dust emission and $C^{18}O$ integrated intensity around NGC 2068 in Orion B allows for an estimation of the temperature within the diffuse cloud. As the temperature of the material increases the dust emission brightens due to the *almost* linear increase in the Planck function; however, for the low lying $C^{18}O$(2-1) line the intensity quickly decreases with temperature as the partition function expands. Mitchell et al. (2001) find that the diffuse gas around NGC 2068 is well represented by a mean temperature of 40 K consistent with the highest temperatures found in Bonnor-Ebert clump analysis above. However, some of the clumps have a significantly higher ratio of dust emission to gas emission. While it is possible to fit these clumps with a much higher temperature it is also possible to consider a lower temperature for the clumps and a freezing out of the CO onto dust grains. Formaldehyde observations, which predict low temperatures for the gas in a handful of observed clumps and spectral index measurements between 450μm and 850μm support the latter explanation (Mitchell et al. 2001).

Determining the physical properties of the clumps and their surroundings should be one of the prime tasks of FIRST. Combining excellent sensitivity and stability of SPIRE, observing the spectral energy distribution of the clumps will be trivial. Further, complete spectral maps obtained with HIFI will determine the chemical properties of the clumps, including the effects of freeze-out and other time dependent reactions. Deep continuum integrations on the inter-clump medium will place constraints on the how the clumps formed and will allow follow-up strategic line surveys.

5. Conclusions

Surveying large regions of nearby molecular clouds in the sub-millimeter has provided new insights into the physical properties at play in star-forming regions. Most importantly the distribution of stellar masses appears to occur at a much earlier phase than anticipated during the formation of pre-collapsing clumps. However, if this result holds it is difficult to understand what provides the mechanism whereby the clumps collapse to stars. FIRST should provide a great deal of additional knowledge, both because it will be able to map much larger regions of space and because it will provide almost complete spectral energy distributions throughout these regions. The real strength of FIRST will be found by complimenting the continuum observations of SPIRE and PACS with extensive coverage of molecular lines using HIFI. Together these instruments should aid in unlocking the many mysteries of star formation that remain.

Acknowledgements

This research is supported through a grant from the Natural Sciences and Engineering Research Council of Canada. I wish to acknowledge my collaborators in the Canadian JCMT key project survey of molecular clouds: L. Avery, S. Basu, M. Fich, J. Fiege, G. Joncas, L. Knee, B. Matthews, H. Matthews, G. Mitchell, G. Moriarty-Schieven, R. Pudritz and C. Wilson. I also thank my Orion A collaborators J. Bally and E. van Dishoeck. The JCMT is operated by the JAC on behalf of PPARC of the UK, the Netherlands OSR, and NRC of Canada.

References

Bally, J., et al. 1987, ApJ 313, L45
Bonnor,W.B.1956, MNRAS 112, 195
Chini, R., et al. 1997, ApJ, 474, L135
Ebert, R. 1955, Zs.Ap. 37, 217
Fiege, J.D. & Pudritz, R.E. 2000a, MNRAS 311, 85
Fiege, J.D. & Pudritz, R.E. 2000b, MNRAS 311,105
Fiege, J.D. & Pudritz, R.E. 2000c, ApJ, 544, 830
Groesbeck, T.D. 1994, Ph.D. thesis, Caltech
Holland, W.S. et al. 1999, MNRAS, 303, 659
Johnstone, D. 2001, in preparation
Johnstone, D. & Bally, J. 1999, ApJ 510, L49
Johnstone, D., et al. 2000a, ApJS 131, 505
Johnstone, D., et al. 2000b, ApJ 545, 327
Johnstone, D.,et al. 2001, ApJ, submitted
Matthews, B.C. & Wilson, C.D. 2000, ApJ, 531, 868
McKee, C.F. 1989, ApJ 345, 782
Mitchell, G., Johnstone, D., et al. 2001, ApJ, submitted
Motte, F., André, P., & Neri, R. 1998, A&A 336, 150
Myers, P.C. & Lazarian, A. 1998, ApJ 507, L157
Ostriker, J. 1964, ApJ 140, 1056
Serabyn, E. & Weisstein, E.W. 1995, ApJ, 451, 238
Testi, L. & Sargent, A.I. 1998, ApJ 508, L91
Williams, J.P., de Geus, E.,J., & Blitz L. 1994, ApJ 428, 693
Wilson, C.D. et al. 1999, ApJ 513, L139
Wiseman, J.J. & Ho, P.T.P. 1998, ApJ 502, 676
Yu, K.C, Bally, J., & Devine, D. 1997, ApJ 485, L45